Mathematics and Visualization

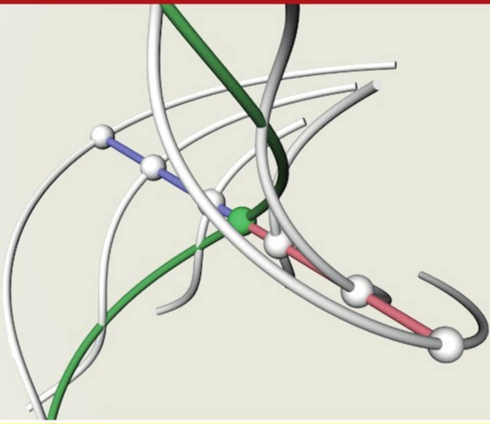

Ronald Peikert Hamish Carr
Helwig Hauser Raphael Fuchs *Editors*

Topological Methods in Data Analysis and Visualization II

Theory, Algorithms, and Applications

Springer

Mathematics and Visualization

For further volumes:
http://www.springer.com/series/4562

Ronald Peikert
Helwig Hauser
Hamish Carr
Raphael Fuchs
Editors

Topological Methods in Data Analysis and Visualization II

Theory, Algorithms, and Applications

Springer

Editors

Ronald Peikert
ETH Zürich
Computational Science
Zürich
Switzerland
peikert@inf.ethz.ch

Hamish Carr
University of Leeds
School of Computing
Leeds
United Kingdom
H.Carr@leeds.ac.uk

Helwig Hauser
University of Bergen
Dept. of Informatics
Bergen
Norway
Helwig.Hauser@UiB.no

Raphael Fuchs
ETH Zürich
Computational Science
Zürich
Switzerland
raphael@inf.ethz.ch

ISBN 978-3-642-23174-2 e-ISBN 978-3-642-23175-9
DOI 10.1007/978-3-642-23175-9
Springer Heidelberg Dordrecht London New York

Library of Congress Control Number: 2011944972

Mathematical Subject Classification (2010): 37C10, 57Q05, 58K45, 68U05, 68U20, 76M27

Printed on acid-free paper

Springer is part of Springer Science+Business Media (www.springer.com)

Preface

Over the past few decades, scientific research became increasingly dependent on large-scale numerical simulations to assist the analysis and comprehension of physical phenomena. This in turn has led to an increasing dependence on scientific visualization, i.e., computational methods for converting masses of numerical data to meaningful images for human interpretation.

In recent years, the size of these data sets has increased to scales which vastly exceed the ability of the human visual system to absorb information, and the phenomena being studied have become increasingly complex. As a result, scientific visualization, and scientific simulation which it assists, have given rise to systematic approaches to recognizing physical and mathematical features in the data.

Of these systematic approaches, one of the most effective has been the use of a topological analysis, in particular computational topology, i.e., the topological analysis of discretely sampled and combinatorially represented data sets. As topological analysis has become more important in scientific visualization, a need for specialized venues for reporting and discussing related research has emerged.

This book results from one such venue: the *Fourth Workshop on Topology Based Methods in Data Analysis and Visualization (TopoInVis 2011)*, which took place in Zürich, Switzerland, on April 4–6, 2011. Originating in Europe with successful workshops in Budmerice, Slovakia (2005), and Grimma, Germany (2007), this workshop became truly international with TopoInVis 2009 in Snowbird, Utah, USA (2009). With 43 participants, TopoInVis 2011 continues this run of successful workshops, and future workshops are planned in both Europe and North America under the auspices of an international steering committee of experts in topological visualization, and a dedicated website at http://www.TopoInVis.org/.

The program of *TopoInVis 2011* included 20 peer-reviewed presentations and two keynote talks given by invited speakers. Martin Rasmussen, Imperial College, London, addressed the ongoing efforts of our community to formulate a vector field topology for unsteady flow. His presentation *An introduction to the qualitative theory of nonautonomous dynamical systems* was highly appreciated as an illustrative introduction into a difficult mathematical subject. The second keynote, *Looking for intuition behind discrete topologies*, given by Thomas Lewiner, PUC-Rio,

Rio de Janeiro, picked up another topic within the focus of current research, namely combinatorial methods, for which his talk gave strong motivation. At the end of the workshop, Dominic Schneider and his coauthors were given the award for the best paper by a jury.

Nineteen of the papers presented at *TopoInVis 2011* were revised and, in a second round of reviewing, accepted for publication in this book. Based on the major topics covered, the papers have been grouped into four parts.

The first part of the book is concerned with computational discrete Morse theory, both in 2D and in 3D. In 2D, Reininghaus and Hotz applied discrete Morse theory to divergence-free vector fields. In contrast, Günther et al. present a combinatorial algorithm to construct a hierarchy of combinatorial gradient vector fields in 3D, while Gyulassy and Pascucci provide an algorithm that computes the distinct cells of the MS complex connecting two critical points. Finally, an interesting contribution is also made by Reich et al. who developed a combinatorial vector field topology in 3D.

In Part 2, hierarchical methods for extracting and visualizing topological structures such as the contour tree and Morse-Smale complex were presented. Weber et al. propose an enhanced method for contour trees that is able to visualize two additional scalar attributes. Harvey et al. introduce a new clustering-based approach to approximate the Morse–Smale complex. Finally, Wagner et al. describe how to efficiently compute persistent homology of cubical data in arbitrary dimensions.

The third part of the book deals with the visualization of dynamical systems, vector and tensor fields. Tricoche et al. visualize chaotic structures in area-preserving maps. The same problem was studied by Sanderson et al. in the context of an application, namely the structure of magnetic field lines in tokamaks, with a focus on the detection of islands of stability. Jadhav et al. present a complete analysis of the possible mappings from inflow boundaries to outflow boundaries in triangular cells. A novel algorithm for pathline placement with controlled intersections is described by Weinkauf et al., while Wiebel et al. propose glyphs for the visualization of nonlinear vector field singularities. As an interesting result in tensor field topology, Lin et al. present an extension to asymmetric 2D tensor fields.

The final part is dedicated to the topological visualization of unsteady flow. Kasten et al. analyze finite-time Lyapunov exponents (FTLE) and propose alternative realizations of Lagrangian coherent structures (LCS). Schindler et al. investigate the flux through FTLE ridges and propose an efficient, high-quality alternative to height ridges. Pobitzer et al. present a technique for detecting and removing false positives in LCS computation. Schneider et al. propose an FTLE-like method capable of handling uncertain velocity data. Sadlo et al. investigate the time parameter in the FTLE definition and provide a lower bound. Finally, Fuchs et al. explore scale-space approaches to FTLE and FTLE ridge computation.

Acknowledgements *TopoInVis 2011* was organized by the Scientific Visualization Group of ETH Zurich, the Visualization Group at the University of Bergen, and the Visualization and Virtual Reality Group at the University of Leeds. We acknowledge the support from ETH Zurich, particularly for allowing us to use the prestigious Semper Aula in the main building. The *Evento* team provided valuable support by setting up the registration web page and promptly resolving issues with on-line payments. We are grateful to Marianna Berger, Katharina Schuppli, Robert Carnecky, and Benjamin Schindler for their administrative and organizational help. We also wish to thank the *TopoInVis* steering committee for their advice and their help with advertising the event. The project *SemSeg–4D Space-Time Topology for Semantic Flow Segmentation* supported TopoInVis 2011 in several ways, most notably by offering 12 young researchers partial refunding of their travel costs. The project SemSeg acknowledges the financial support of the Future and Emerging Technologies (FET) programme within the Seventh Framework Programme for Research of the European Commission, under FET-Open grant number 226042.

We are looking forward to the next *TopoInVis* workshop, which is planned to take place in 2013 in North America.

Ronald Peikert
Helwig Hauser
Hamish Carr
Raphael Fuchs

Contents

Part I
Discrete Morse Theory

Computational Discrete Morse Theory for Divergence-Free 2D Vector Fields

Jan Reininghaus and Ingrid Hotz

1 Introduction

We introduce a robust and provably consistent algorithm for the topological analysis of divergence-free 2D vector fields.

Topological analysis of vector fields has been introduced to the visualization community in [10]. For an overview of recent work in this field we refer to Sect. 2. Most of the proposed algorithms for the extraction of the topological skeleton try to find all zeros of the vector field numerically and then classify them by an eigenanalysis of the Jacobian at the respective points. This algorithmic approach has many nice properties like performance and familiarity. Depending on the data and the applications there are however also two shortcomings.

1.1 Challenges

If the vector field contains plateau like regions, i.e. regions where the magnitude is rather small, these methods have to deal with numerical problems and may lead to topologically inconsistent results. This means that topological skeletons may be computed that cannot exist on the given domain. A simple example for this problem can be given in 1D. Consider an interval containing exactly three critical points as shown in Fig. 1a. While it is immediately clear that not all critical points can be of the same type, an algorithm that works strictly locally using numerical algorithms may result in such an inconsistent result. A second problem that often arises is that

J. Reininghaus (✉) · I. Hotz
Zuse Institute Berlin, Takustr. 7, 14195 Berlin, Germany
e-mail: reininghaus@zib.de; hotz@zib.de

R. Peikert et al. (eds.), *Topological Methods in Data Analysis and Visualization II*, Mathematics and Visualization, DOI 10.1007/978-3-642-23175-9_1,

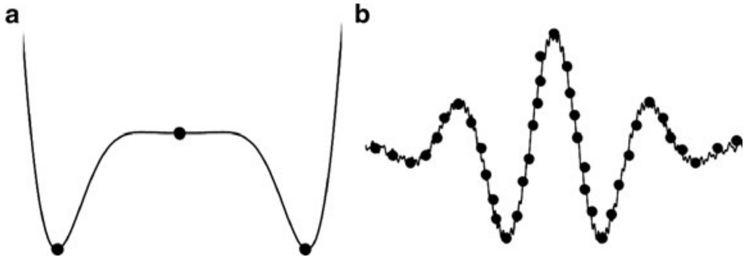

Fig. 1 Illustration of the algorithmic challenges. (**a**) shows 1D function with a plateau-like region. From the topological point of view the critical point in the middle needs to be a maximum since it is located between the two minima on the left and on the right side. However, depending on the numerical procedure the determination of its type might be inconsistent. (**b**) illustrates a noisy 1D function. Every fluctuation caused by the noise generates additional minima and maxima

of noise in the data. Depending on its type and quantity, a lot of spurious critical points may be produced as shown in Fig. 1b. Due to the significance of this problem in practice, a lot of work has been done towards robust methods that can deal with such data, see Sect. 2.

1.2 Contribution

This paper proposes an application of computational discrete Morse theory for divergence-free vector fields. The resulting algorithm for the topological analysis of such vector fields has three nice properties:

1. It provably results in a set of critical points that is consistent with the topology of the domain. This means that the algorithm cannot produce results that are inadmissible on the given domain. The consistency of the algorithm greatly increases its robustness as it can be interpreted as an error correcting code. We will give a precise definition of topological consistency for divergence-free vector fields in Sect. 3.
2. It allows for a simplification of the set of critical points based on an importance measure related to the concept of persistence [5]. Our method may therefore be used to extract the structurally important critical points of a divergence-free vector field and lends itself to the analysis of noisy data sets. The importance measure has a natural physical interpretation and is described in detail in Sect. 4.
3. It is directly applicable to vector fields with only near zero divergence. These fields often arise when divergence-free fields are numerically approximated or measured. This property in demonstrated in Sect. 5.

2 Related Work

Vector field topology was introduced to the visualization community by Helman and Hesselink [11]. They defined the concept of a topological skeleton consisting of critical points and connecting separatrices to segment the field into regions of topologically equivalent streamline behavior. A good introduction to the concepts and algorithms of vector field topology is given in [30], while a systematic survey of recent work in this field can be found in [15].

As the topological skeleton of real world data sets is usually rather complex, a lot of work has been done towards simplification of topological skeletons of vector fields, see [14, 28, 29, 31].

To reduce the dependence of the algorithms on computational parameters like step sizes, a combinatorial approach to vector field topology based on Conley index theory has been developed [3, 4]. In the case of divergence-free vector fields their algorithm unfortunately encounters many problems in practice.

For scalar valued data, algorithms have been developed [1, 8, 13, 16, 25] using concepts from discrete Morse theory [7] and persistent homology [5]. The basic ideas in these algorithms have been generalized to vector valued data in [23, 24] based on a discrete Morse theory for general vector fields [6]. This theory however is not applicable for divergence-free vector fields since it does not allow for center-like critical points. Recently, a unified framework for the analysis of vector fields and gradient vector fields has been proposed in [22] under the name computational discrete Morse theory.

Since vector field data is in general defined in a discrete fashion, a discrete treatment of the differential concepts that are necessary in vector field topology has been shown to be beneficial in [21, 27]. They introduced the idea that the critical points of a divergence-free vector field coincide with the extrema of the scalar potential of the point-wise-perpendicular field to the visualization community. The critical points can therefore be extracted by reconstructing this scalar potential and extracting its minima, maxima, and saddle points. In contrast to our algorithm, their approach does not exhibit the three properties mentioned in Sect. 1.

3 Morse Theory for Divergence-Free 2D Vector Fields

This section shows how theorems from classical Morse theory can be applied in the context of 2D divergence-free vector fields.

3.1 Vector Field Topology

A 2D vector field v is called divergence-free if $\nabla \cdot v = 0$. This class of vector fields often arises in practice, especially in the context of computational fluid dynamics.

For example, the vector field describing the flow of an incompressible fluid, like water, is in general divergence-free. The points at which a vector field v is zero are called the critical points of v. They can be classified by an eigenanalysis of the Jacobian Dv at the respective critical point. In the case of divergence-free 2D vector fields one usually distinguishes two cases [10]. If both eigenvalues are real, then the critical point is called a saddle. If both eigenvalues are imaginary, then the critical point is called a center. Note that one can classify a center furthermore into clockwise rotating (CW-center) or counter-clockwise rotating (CCW-center) by considering the Jacobian as a rotation.

One consequence of the theory that will be presented in this section is that the classification of centers into CW-centers and CCW-centers is essential from a topological point of view. One can even argue that this distinction is as important as differentiating between minima and maxima when dealing with gradient vector fields.

3.2 Morse Theory

The critical points of a vector field are often called topological features. One justification for this point of view is given by Morse theory [17]. Loosely speaking, Morse theory relates the set of critical points of a vector field to the topology of the domain. For example, it can be proven that every continuous vector field on a sphere contains at least one critical point. To make things more precise we restrict ourselves to gradient vector fields defined on a closed oriented surface. The ideas presented below work in principal also for surfaces with boundary, but the notation becomes more cumbersome. To keep things simple, we therefore assume that the surface is closed. We further assume that all critical points are first order, i.e. the Jacobian has full rank at each critical point. Let c_0 denote the number of minima, c_1 the number of saddles, c_2 the number of maxima, and g the genus of the surface. We then have the Poincaré-Hopf theorem

$$c_2 - c_1 + c_0 = 2 - 2g, \tag{1}$$

the weak Morse inequalities

$$c_0 \geq 1, \qquad c_1 \geq 2g, \qquad c_2 \geq 1, \tag{2}$$

and the strong Morse inequality

$$c_1 - c_0 \geq 2g - 1. \tag{3}$$

3.3 Helmholtz-Hodge Decomposition

To apply these theorems from Morse theory to a divergence-free vector field v we can make use of the Helmholtz-Hodge decomposition [12]. Let $\nabla \times \psi = (\partial_y \psi, -\partial_x \psi)$ denote the curl operator in 2D. We then have the orthogonal decomposition

$$v = \nabla \phi + \nabla \times \psi + h. \tag{4}$$

We can thereby uniquely decompose v into an irrotational part $\nabla \phi$, a solenoidal part $\nabla \times \psi$, and a harmonic part h, i.e. $\Delta h = 0$. Due to the assumption that the surface is closed, the space of harmonic vector fields coincides with the space of vector fields with zero divergence and zero curl [26]. Since v is assumed to be divergence-free we have $0 = \nabla \cdot v = \nabla \cdot \nabla \phi$ which implies $\phi = 0$ due to (4). The harmonic-free part $\hat{v} = v - h$ can therefore be expressed as the curl of a scalar valued function

$$\hat{v} = \nabla \times \psi. \tag{5}$$

3.4 Stream Function

The function ψ is usually referred to as the stream function [19]. Let $\hat{v}^{\perp} = (v_2, -v_1)$ denote the point-wise perpendicular vector field of $\hat{v} = (v_1, v_2)$. The gradient of the stream function is then given by

$$\nabla \psi = \hat{v}^{\perp}. \tag{6}$$

Note that $\hat{v}$ has the same set of critical points as $\hat{v}^{\perp}$. The type of its critical points is however changed: CW-center become minima, and CCW-center become maxima. Since (6) shows that $\hat{v}^{\perp}$ is a gradient vector field, we can use this identification to see how (1)–(3) can be applied to the harmonic-free part of divergence-free 2D vector fields.

3.5 Implications

The dimension of the space of harmonic vector fields is given by $2g$ [26]. A vector field defined on a surface which is homeomorphic to a sphere is therefore always harmonic-free, i.e. $\hat{v} = v$. Every divergence-free vector field on a sphere which only contains first order critical points therefore satisfies (1)–(3). For example, every such vector field contains at least one CW-center and one CCW-center.

Due to the practical relevance in Sect. 5 we note that every divergence-free vector field defined on a contractible surface can be written as the curl of a stream function ψ as shown by the Poincaré-Lemma. For such cases, the point-wise perpendicular vector field can therefore also be directly interpreted as the gradient of the stream function.

4 Algorithmic Approach

4.1 Overview

We now describe how we can apply computational discrete Morse theory to divergence-free vector fields. Let v denote a divergence-free vector field defined on an oriented surface S. The first step is to compute the harmonic-free part $\hat{v}$ of v. If S is contractible or homeomorphic to a sphere, then v is itself the curl of a stream function ψ, i.e. $\hat{v} = v$. Otherwise, we need to compute the Helmholtz-Hodge decomposition (4) of v to get its harmonic part. To do this, one can employ the algorithms described in [20, 21, 27].

We now make use of the fact that the point-wise perpendicular vector field $\hat{v}^{\perp}$ has the same critical points as $\hat{v}$. Due to (5), we know that $\hat{v}^{\perp}$ is a gradient vector field. To compute and classify the critical points of the divergence-free vector field $\hat{v}$ it therefore suffices to analyze the gradient vector field $\hat{v}^{\perp}$.

One approach to analyze the gradient vector field $\hat{v}^{\perp}$ would be to compute a scalar valued function ψ such that $\hat{v}^{\perp} = \nabla\psi$. One can then apply one of the algorithms mentioned in Sect. 2 to extract a consistent set of critical points. In this paper, we will apply an algorithm from computational discrete Mose theory to directly analyze the gradient vector field $\hat{v}^{\perp}$. The main benefit of this approach is that it allows us to consider $\hat{v}^{\perp}$ as a gradient vector field even if it contains a small amount of curl. This is a common problem in practice, since a numerical approximation or measurement of a divergence-free field often contains a small amount of divergence. By adapting the general approach presented in [22], we can directly deal with such fields with no extra pre-processing steps. Note that the importance measure for the critical points of a gradient vector field has a nice physical interpretation in the case of rotated stream functions. This will be explained in more detail below.

4.2 Computational Discrete Morse Theory

The basic idea in computational discrete Morse theory is to consider Forman's discrete Morse theory [7] as a discretization of the admissible extremal structures of a given surface. The extremal structure of a scalar field consists of critical points and separatrices – the integral lines of the gradient field that connect the critical points. Using this description of the topologically consistent structures we then define an optimization problem that results in a hierarchy of extremal structures that represents the given input data with decreasing level of detail.

4.2.1 Definitions

Let C denote a finite regular cell complex [9] that represents the domain of the given vector field. Examples of such cell complexes that arise in practice are triangulations or quadrangular meshes. We first define its cell graph $G = (N, E)$, which encodes the combinatorial information contained in C in a graph theoretic setting.

The nodes N of the graph consist of the cells of the complex C and each node u^p is labeled with the dimension p of the cell it represents. The edges E of the graph encode the neighborhood relation of the cells in C. If the cell u^p is in the boundary of the cell w^{p+1}, then $e^p = \{u^p, w^{p+1}\} \in E$. We refer to Fig. 2a for an example of a simple cell graph. Note that we additionally label each edge with the dimension of its lower dimensional node.

A subset of pairwise non-adjacent edges is called a matching. Using these definitions, a combinatorial vector field V on a regular cell complex C can be defined as a matching of the cell graph G, see Fig. 2a for an example. The set of combinatorial vector fields on C is thereby given by the set of matchings $\mathscr{M}$ of the cell graph G.

We now define the extremal structure of a combinatorial vector field. The unmatched nodes are called critical points. If u^p is a critical point, we say that the critical point has index p. A critical point of index p is called sink ($p = 0$), saddle ($p = 1$), or source ($p = 2$). A combinatorial p-streamline is a path in the graph whose edges are of dimension p and alternate between V and its complement. A p-streamline connecting two critical points is called a p-separatrix. If a p-streamline is closed, we call it either an attracting periodic orbit ($p = 0$) or a repelling periodic orbit ($p = 1$). For examples of these combinatorial definitions of the extremal structure we refer to Figs. 2b–d.

As shown in [2], a combinatorial gradient vector field V^ϕ can be defined as a combinatorial vector field that contains no periodic orbits. A matching of G that gives rise to such a combinatorial vector field is called a Morse matching. The set of combinatorial gradient vector fields on C is therefore given by the set of Morse matchings $\mathscr{M}$ of the cell graph G. In the context of gradient vector fields, we refer to a critical point u^p as a minimum ($p = 0$), saddle ($p = 1$), or maximum ($p = 2$).

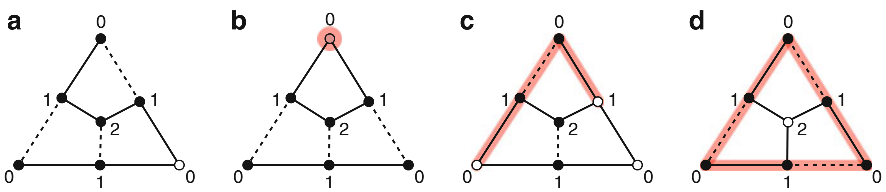

Fig. 2 Basic definitions. (**a**) a combinatorial vector field (*dashed*) on the cell graph of a single triangle. The numbers correspond to the dimension of the represented cells, and matched nodes are drawn solid. (**b**) a critical point of index 0. (**c**) a 0-separatrix. (**d**) an attracting periodic orbit

We now compute edge weights $\omega : E \to \mathbb{R}$ to represent the given vector field $\hat{v}^{\perp}$. The idea is to assign a large weight to an edge $e^p = \{u^p, w^{p+1}\}$ if an arrow pointing from u^p to w^{p+1} represents the flow of $\hat{v}^{\perp}$ well. The weight for e^p is therefore computed by integrating the tangential component of the vector field $\hat{v}^{\perp}$ along the edge e^p.

4.2.2 Computation

We can now define the optimization problem

$$V_k^{\phi} = \arg \max_{M \in \mathscr{M}^{\phi}, |M|=k} \omega(M). \tag{7}$$

Let $k_0 = \arg\max_{k \in \mathbb{N}} \omega(V_k)$ denote the size of the maximum weight matching, and let $k_n = \max_{k \in \mathbb{N}} |V_k|$ denote the size of the heaviest maximum cardinality matching. The hierarchy of combinatorial gradient vector fields that represents the given vector field $\hat{v}^{\perp}$ with decreasing level of detail is now given by

$$\mathscr{V}^{\phi} = \left(V_k^{\phi}\right)_{k=k_0,\ldots,k_n}. \tag{8}$$

For a fast approximation algorithm for (8) and the extraction of the extremal structure of a particular combinatorial gradient vector field we refer to [22].

4.2.3 Importance Measure

Note that the sequence (8) is ordered by an importance measure which is closely related to homological persistence [5]. The importance measure is defined by the height difference of a certain pairing of critical points. Since we are dealing with the gradient of a stream function of a divergence-free vector field there is a nice physical interpretation of this value. The height difference between two points of the stream function is the same as the amount of flow passing through any line connecting the two points [19]. This allows us to differentiate between spurious and structurally important critical points in divergence-free 2D vector fields, as will be demonstrated in the next section.

5 Examples

The purpose of this section is to provide some numerical evidence for the properties of our method mentioned in Sect. 1. The running time of our algorithm is 47 s for a surface with one million vertices using an Intel Core i7 860 CPU with 8 GB RAM.

5.1 Noise Robustness

To illustrate the robustness of our algorithm with respect to noise, we sampled the divergence-free vector field

$$v(x, y) = \nabla \times \left(\sin(6\,x)\ \sin(6\,y)\, e^{-3\,(x^2+y^2)}\right) \tag{9}$$

on the domain $[-1, 1]^2$ with a uniform 512^2 grid. A LIC image of this divergence-free vector field is shown in Fig. 3, left. To simulate a noisy measurement of this vector field, we added uniform noise with a range of $[-1, 1]$ to this data set. A LIC image of the resulting quasi-divergence-free vector field is shown in Fig. 3, right. Since the square is a contractible domain, we can directly apply the algorithm described in Sect. 4 to both data sets and extracted the 23 most important critical points. As can be seen in Fig. 3, our method is able to effectively deal with the noisy data.

5.2 Importance Measure

To illustrate the physical relevance of the importance measure for the extracted critical points we consider a model example from computational fluid dynamics [18]. Figure 4, top, shows a LIC image of a simulation of the flow behind a circular cylinder – the cylinder is on the left of the shown data set. Since we are considering only a contractible subset of the data set, we can directly apply the algorithm described in Sect. 4. Note that due to a uniform sampling of this data set a small amount of divergence was introduced. The divergence is depicted in Fig. 4, bottom.

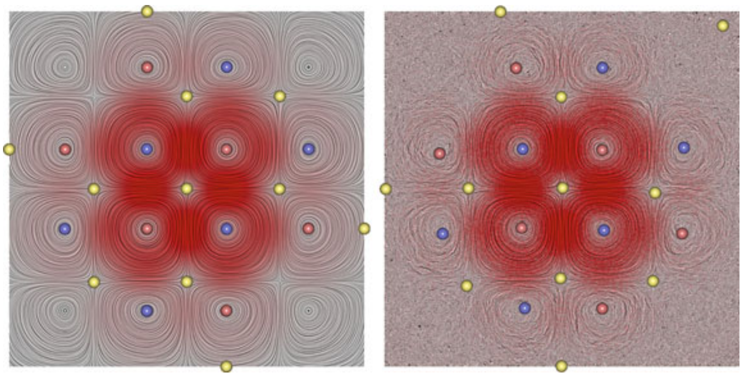

Fig. 3 A synthetic divergence-free vector field is depicted using a LIC image colored by magnitude. The critical points of $V^{\phi}_{k_n-11}$ are shown. The saddles, CW-centers, and CCW-centers are depicted as *yellow*, *blue*, and *red* spheres. *Left*: the original smooth vector field. *Right*: a noisy measurement of the field depicted on the left

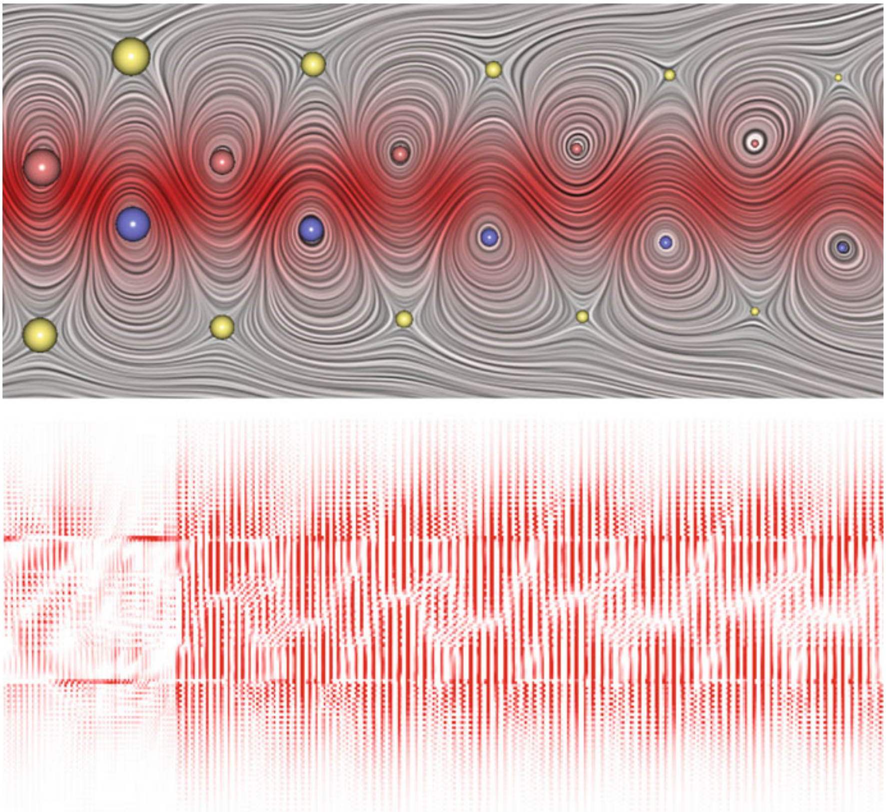

Fig. 4 *Top*: A quasi-divergence-free vector field of the flow behind a circular cylinder is depicted using a LIC image colored by magnitude. The saddles, CW-centers, and CCW-centers are depicted as *yellow*, *blue*, and *red* spheres and are scaled by our importance measure. *Bottom*: the divergence of the data set is shown using a colormap (*white*: zero divergence, *red*: high divergence)

The data set exhibits the well-known Kármán vortex street of alternating clockwise and counter-clockwise rotating vortices. This structure is extracted well by our algorithm. The strength of the vortices decreases the further they are from the cylinder on the left. This physical property is reflected well by our importance measure for critical points in divergence-free vector fields.

6 Conclusion

We presented an algorithm for the extraction of critical points in 2D divergence-free vector fields. In contrast to previous work this algorithm is provably consistent in the sense of Morse theory for divergence-free vector fields as presented in Sect. 3.

It also allows for a consistent simplification of the set of critical points which enables the analysis of noisy data as illustrated in Fig. 3. The computed importance measure has a physical relevance as shown in Fig. 4, and allows to discriminate between dominant and spurious critical points in a data set. By combinatorially enforcing the gradient vector field property we are able to directly deal with data sets with only near zero divergence (see Fig. 4, bottom).

The only step of our algorithm that is not combinatorial is the Helmholtz-Hodge decomposition which is necessary for surfaces of higher genus to get the harmonic-free part of the vector field. It would therefore be interesting to investigate the possibility of a purely combinatorial Helmholtz-Hodge decomposition. Alternatively, one could try to develop a computational discrete Morse theory for divergence-free vector fields containing a harmonic part.

Acknowledgements We would like to thank David Günther, Jens Kasten, and Tino Weinkauf for many fruitful discussions on this topic. This work was funded by the DFG Emmy-Noether research programm. All visualizations in this paper have been created using AMIRA – a system for advanced visual data analysis (see http://amira.zib.de/).

References

1. Bauer, U., Lange, C., Wardetzky, M.: Optimal topological simplification of discrete functions on surfaces. arXiv:1001.1269v2 (2010)
2. Chari, M.K.: On discrete Morse functions and combinatorial decompositions. Discrete Math. **217**(1-3), 101–113 (2000)
3. Chen, G., Mischaikow, K., Laramee, R., Pilarczyk, P., Zhang, E.: Vector field editing and periodic orbit extraction using Morse decomposition. IEEE Trans. Visual. Comput. Graph. **13**, 769–785 (2007)
4. Chen, G., Mischaikow, K., Laramee, R.S., Zhang, E.: Efficient morse decomposition of vector fields. IEEE Trans. Visual. Comput. Graph. **14**(4), 848–862 (2008)
5. Edelsbrunner, H., Letscher, D., Zomorodian, A.: Topological persistence and simplification. Discrete Comput. Geom. **28**, 511–533 (2002)
6. Forman, R.: Combinatorial vector fields and dynamical systems. Mathematische Zeitschrift **228**(4), 629–681 (1998)
7. Forman, R.: Morse theory for cell complexes. Adv. Math. **134**, 90–145 (1998)
8. Gyulassy, A.: Combinatorial Construction of Morse-Smale Complexes for Data Analysis and Visualization. PhD thesis, University of California, Davis (2008)
9. Hatcher, A.: Algebraic Topology. Cambridge University Press, Cambridge, U.K. (2002)
10. Helman, J., Hesselink, L.: Representation and display of vector field topology in fluid flow data sets. IEEE Comput. **22**(8), 27–36 (1989)
11. Helman, J., Hesselink, L.: Representation and display of vector field topology in fluid flow data sets. Computer **22**(8), 27–36 (1989)
12. Helmholtz, H.: Über integrale der hydrodynamischen gleichungen, welche den wirbelbewegungen entsprechen. J. Reine Angew. Math. **55**, 25–55 (1858)
13. King, H., Knudson, K., Mramor, N.: Generating discrete Morse functions from point data. Exp. Math. **14**(4), 435–444 (2005)
14. Klein, T., Ertl, T.: Scale-space tracking of critical points in 3d vector fields. In: Helwig Hauser, H.H., Theisel, H. (eds.) Topology-based Methods in Visualization, Mathematics and Visualization, pp. 35–49. Springer, Berlin (2007)

15. Laramee, R.S., Hauser, H., Zhao, L., Post, F.H.: Topology-based flow visualization, the state of the art. In: Helwig Hauser, H.H., Theisel, H. (eds.) Topology-based Methods in Visualization, Mathematics and Visualization, pp. 1–19. Springer, Berlin (2007)
16. Lewiner, T.: Geometric discrete Morse complexes. PhD thesis, Department of Mathematics, PUC-Rio, 2005. Advised by Hélio Lopes and Geovan Tavares.
17. Milnor, J.: Morse Theory. Princeton University Press, Princeton (1963)
18. Noack, B.R., Schlegel, M., Ahlborn, B., Mutschke, G., Morzyński, M., Comte, P., Tadmor, G.: A finite-time thermodynamics of unsteady fluid flows. J. Non-Equilibr. Thermodyn. **33**(2), 103–148 (2008)
19. Panton, R.: Incompressible Flow. Wiley, New York (1984)
20. Petronetto, F., Paiva, A., Lage, M., Tavares, G., Lopes, H., Lewiner, T.: Meshless Helmholtz-Hodge decomposition. Trans. Visual. Comput. Graph. **16**(2), 338–342 (2010)
21. Polthier, K., Preuß, E.: Identifying vector field singularities using a discrete Hodge decomposition. pp. 112–134. Springer, Berlin (2002)
22. Reininghaus, J., Günther, D., Hotz, I., Prohaska, S., Hege, H.-C.: TADD: A computational framework for data analysis using discrete Morse theory. In: Fukuda, K., van der Hoeven, J., Joswig, M., Takayama, N. (eds.) Mathematical Software – ICMS 2010, volume 6327 of Lecture Notes in Computer Science, pp. 198–208. Springer, Berlin (2010)
23. Reininghaus, J., Hotz, I.: Combinatorial 2d vector field topology extraction and simplification. In: Pascucci, V., Tricoche, X., Hagen, H., Tierny, J. (eds.) Topological Methods in Data Analysis and Visualization, Mathematics and Visualization, pp. 103–114. Springer, Berlin (2011)
24. Reininghaus, J., Löwen, C., Hotz, I.: Fast combinatorial vector field topology. IEEE Trans. Visual. Comput. Graph. **17** 1433–1443 (2011)
25. Robins, V., Wood, P.J., Sheppard, A.P.: Theory and algorithms for constructing discrete morse complexes from grayscale digital images. IEEE Trans. Pattern Anal. Mach. Learn. **33**(8), 1646–1658 (2011)
26. Shonkwiler, C.: Poincaré duality angles for Riemannian manifolds with boundary. Technical Report arXiv:0909.1967, Sep 2009. Comments: 51 pages, 6 figures.
27. Tong, Y., Lombeyda, S., Hirani, A.N., Desbrun, M.: Discrete multiscale vector field decomposition. In: ACM Transactions on Graphics (TOG) - Proceedings of ACM SIGGRAPH, volume 22 (2003)
28. Tricoche, X., Scheuermann, G., Hagen, H.: Continuous topology simplification of planar vector fields. In: VIS '01: Proceedings of the conference on Visualization '01, pp. 159–166. IEEE Computer Society, Washington, DC, USA (2001)
29. Tricoche, X., Scheuermann, G., Hagen, H., Clauss, S.: Vector and tensor field topology simplification on irregular grids. In: Ebert, D., Favre, J.M., Peikert, R. (eds.) VisSym '01: Proceedings of the symposium on Data Visualization 2001, pp. 107–116. Springer, Wien, Austria, May 28–30 (2001)
30. Weinkauf, T.: Extraction of Topological Structures in 2D and 3D Vector Fields. PhD thesis, University Magdeburg (2008)
31. Weinkauf, T., Theisel, H., Shi, K., Hege, H.-C., Seidel, H.-P.: Extracting higher order critical points and topological simplification of 3D vector fields. In: Proceedings IEEE Visualization 2005, pp. 559–566. Minneapolis, U.S.A., October 2005

Efficient Computation of a Hierarchy of Discrete 3D Gradient Vector Fields

David Günther, Jan Reininghaus, Steffen Prohaska, Tino Weinkauf, and Hans-Christian Hege

1 Introduction

The analysis of three dimensional scalar data has become an important tool in scientific research. In many applications, the analysis of topological structures – the critical points, separation lines and surfaces – are of great interest and may help to get a deeper understanding of the underlying problem. Since these structures have an extremal characteristic, we call them *extremal structures* in the following.

The extremal structures have a long history [2, 14]. Typically, the critical points are computed by finding all zeros of the gradient, and can be classified into minima, saddles, and maxima by the eigenvalues of their Hessian. The respective eigenvectors can be used to compute the separation lines and surfaces as solutions of autonomous ODEs. For the numerical treatment of these problems we refer to Weinkauf [22].

One of the problems that such numerical algorithms face is the discrete nature of the extremal structures. For example, the type of a critical point depends on the signs of the eigenvalues. If the eigenvalues are close to zero, the determination of the type is ill-posed and numerically challenging. Depending on the input data, the resulting extremal structure may therefore strongly depend on the algorithmic parameters and numerical procedures. From a topological point of view, this can be quite problematic. Morse theory relates the extremal structure of a generic function to the topology of the manifold, e.g., by the Poincaré-Hopf Theorem or by the

D. Günther (✉), J. Reininghaus, S. Prohaska, H.-C. Hege
Zuse Institute Berlin, Takustr. 7, 14195 Berlin, Germany
e-mail: david.guenther@zib.de; reininghaus@zib.de; prohaska@zib.de; hege@zib.de

T. Weinkauf
Courant Institute of Mathematical Sciences, New York University, 715 Broadway, New York, NY 10003, U.S.A
e-mail: weinkauf@courant.nyu.edu

R. Peikert et al. (eds.), *Topological Methods in Data Analysis and Visualization II*, Mathematics and Visualization, DOI 10.1007/978-3-642-23175-9_2,

strong Morse inequalities [15]. The topology of the manifold restricts the set of the admissible extremal structures.

Another problem is the presence of noise, for example due to the imaging process, or sampling artifacts. Both can create fluctuations in the scalar values that may create additional extremal structures, which are very complex and hard to analyze, in general. A distinction between important and spurious elements is thereby crucial.

To address these problems, one may use the framework of discrete Morse theory introduced by Forman who translated concepts from continuous Morse theory into a discrete setting for cell complexes [5]. A gradient field is encoded in the combinatorial structure of the cell complex, and its extremal structures are defined in a combinatorial fashion. A finite cell complex can therefore carry only a finite number of combinatorial gradient vector fields, and their respective extremal structures are always consistent with the topology of the manifold.

The first computational realization of Forman's theory was presented by Lewiner et al. [12, 13] to compute the homology groups of 2D and 3D manifolds. In this framework, a sequence of consistent combinatorial gradient fields can be computed such that the underlying extremal structures become less complex with respect to some importance measure. The combinatorial fields are represented by hypergraphs and hyperforests, which allow for a very compact and memory efficient representation of the extremal structure. However, the framework is only applicable to relatively small three dimensional data sets since the construction of the sequence requires several graph traversals. This results in a non-feasible running time for large data sets. Recently, several alternatives for the computation of a discrete Morse function were proposed, for example by Robins et al. [18] and King et al. [11].

An alternative approach to extract the essential critical points and separation lines was proposed by Gyulassy [7]. His main idea is to construct a single initial field and extract its complex extremal structures by a field traversal. To separate spurious elements from important ones, the extremal structures are then directly simplified. One advantage of this approach is a very low running time. One drawback is that certain pairs of critical points, i.e., the saddle points, may be connected among each other arbitrarily often by saddle connectors [21]. This can result in a large memory overhead [8] since the connectors as well as their geometric embedding need to be stored separately. Note that the reconstruction of a combinatorial gradient vector field based only on a set of critical points and their separation lines is challenging.

In this work, we construct a nested sequence of combinatorial gradient fields. The extremal structures are therein implicitly defined, which enables a memory-efficient treatment of these structure. Additionally, the complete combinatorial flow is preserved at different levels of detail, which allows not only the extraction of separation surfaces, but may also be useful for the analysis of 3D time-dependent data as illustrated by Reininghaus et al. [17] for 2D.

The computation of our sequence is based on the ideas of Reininghaus et al. [16]. A combinatorial gradient field is represented by a Morse matching in a derived cell graph. In this paper, we focus on scalar data given on a 3D structured grid.

Although the computation of a sequence of Morse matchings is a global problem, an initial Morse matching can be computed locally and in parallel. We use an OpenMP implementation of the *ProcessLowerStar*-algorithm proposed by Robins et al. [18] to compute this initial matching. The critical points in this matching correspond one-to-one to the changes of the topology of the lower level cuts of the input data.

As mentioned earlier, the presence of noise may lead to a very complex initial extremal structure. The objective of this paper is to efficiently construct a nested sequence of Morse matchings such that every element of this sequence is topologically consistent, and the underlying extremal structures become less complex in terms of number of critical points. The ordering of the sequence is based on an importance measure that is closely related to the persistence measure [4, 24], and is already successfully used by Lewiner [12] and Gyulassy [7]. This measure enables the selection of a Morse matching with a prescribed complexity of the extremal structure in a very fast, almost interactive post-processing step. The critical points and the separation lines and surfaces are then easily extracted by collecting all unmatched nodes in the graph and a constrained depth-first search starting at these nodes.

The rest of the paper is organized as follows: in Sect. 2, we formulate elements of discrete More theory in graph theoretical terms. In Sect. 3, we present our new algorithm for constructing a hierarchy of combinatorial gradient vector fields. In Sect. 4, we present some examples to illustrate the result of our algorithm and its running time.

2 Computational Discrete Morse Theory

This section begins with a short introduction to discrete Morse theory in a graph theoretical formulation. We then recapitulate the optimization problem that results in a hierarchy of combinatorial gradient vector fields representing a 3D image data set. For simplicity, we restrict ourselves to three dimensional scalar data given on the vertices of a uniform regular grid. The mathematical theory for combinatorial gradient vector fields, however, is defined in a far more general setting [5].

2.1 Cell Graph

Let C denote a finite regular cell complex [9] defined by a 3D grid. In this paper, we call a cell complex *regular* if the boundary of each d-cell is contained in a union of $(d-1)$-cells. The cell graph $G = (N, E)$ encodes the combinatorial information

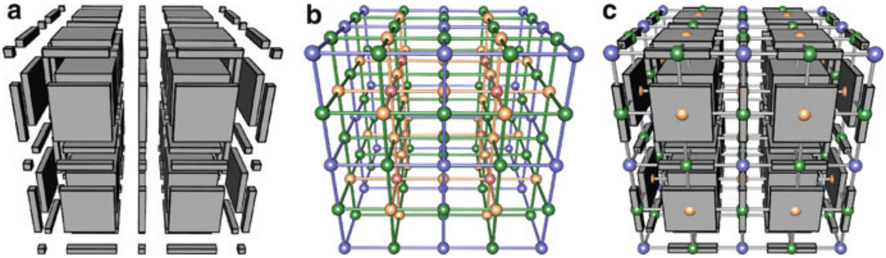

Fig. 1 Illustration of a cell complex and its derived cell graph. (**a**) shows the cells of a $2 \times 2 \times 2$ uniform grid in an exploded view. A single voxel is represented by eight 0-cells, twelve 1-cells, six 2-cells, and one 3-dimensional cell. These cells and their boundary relation define the cell complex. (**b**) shows the derived cell graph. The nodes representing the 0-, 1-, 2-, and 3-cells are shown as *blue*, *green*, *yellow* and *red spheres* respectively. The adjacency of the nodes is given by the boundary relation of the cells. The edges are colored by the lower dimensional incident node. (**c**) shows the cell complex and the cell graph to illustrate the neighborhood relation of the cells

contained in C. The nodes N of the graph consist of the cells of the complex C and each node u^p is labeled with the dimension p of the cell it represents. The scalar value of each node is also stored. Higher dimensional nodes are assigned the maximal scalar value of the incident lower dimensional nodes. The edges E of the graph encode the neighborhood relation of the cells in C. If the cell u^p is in the boundary of the cell w^{p+1}, then $e^p = \{u^p, w^{p+1}\} \in E$. We label each edge with the dimension of its lower dimensional node. An illustration of a cell complex and its graph is shown in Fig. 1. Note that the node indices, their adjacence and their geometric embedding in $\mathbb{R}^3$ are given implicitly by the grid structure.

2.2 *Morse Matchings*

A subset of pairwise non-adjacent edges is called a *matching* $M \subset E$. Using these definitions, a *combinatorial gradient vector field* V on a regular cell complex C can be defined as a certain acyclic matching of the cell graph G [3]. The set of combinatorial gradient vector fields on C is given by the set of these matchings, i.e., the set of *Morse matchings* $\mathscr{M}^\phi$ of the cell graph G. An illustration of a 2D Morse matching is shown in Fig. 2a.

2.3 *Extremal Structures*

We now define the extremal structures of a combinatorial gradient vector field V in G. The unmatched nodes are called *critical nodes*. If u^p is a critical node, we say that the critical node has index p. A *critical node* of index p is called

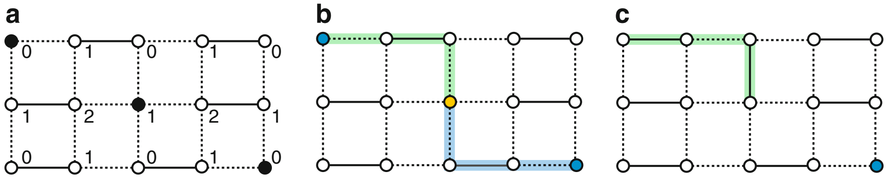

Fig. 2 Depiction of algorithm *constructHierarchy*. Image (**a**) shows a $2D$ Morse matching M. The matched and unmatched edges of the cell graph G are depicted as *solid* and *dashed lines* respectively. The unmatched nodes of G are shown as *black dots*. Each node of G is labeled by its dimension. Image (**b**) shows the two minima (*blue dots*) and the saddle (*yellow dot*) as well as the only two possible augmenting paths (*blue and green stripes*) in M. Image (**c**) shows the augmentation of M along the left (*green*) path. The start- and endnode of this path are now matched and not critical anymore. A single minimum (*blue dot*) remains in M

minimum ($p = 0$), 1-saddle ($p = 1$), 2-saddle ($p = 2$), or maximum ($p = 3$). A combinatorial *p-streamline* is a path in the graph whose edges are of dimension p and alternate between $V \subset E$ and its complement $E \setminus V$. In a Morse matching, there are no closed p-streamlines. This defines the acyclic constraint for Morse matchings. A p-streamline connecting two critical nodes is called a *p-separation line*. A *p-separation surface* is given by all combinatorial 1-streamlines that emanate from a critical point of index p. The extremal structures give rise to a Morse-Smale complex that represents the topological changes in the level sets of the input data. Since we have assigned the maximal value to higher dimensional cells, there are no saddles with a scalar value smaller or greater than their connected minima or maxima respectively.

2.4 Optimization Problem

The construction of a hierarchy can be formulated as an optimization problem [16]. Given edge weights $\omega : E \to \mathbb{R}$, the objective is to find an acyclic matching $V_k \in \mathscr{M}^\phi$ such that

$$V_k = \underset{M \in \mathscr{M}^\phi,\, |M|=k}{\arg\max}\ \omega(M). \tag{1}$$

However, (1) becomes an NP-hard problem in the case of 3D manifolds [10]. We therefore only use (1) to guide our algorithmic design to construct a nested sequence of combinatorial gradient vector fields $\mathscr{V} = (V_k)_{k=k_0,\ldots,k_n}$. For each k, we are looking for the smallest fluctuation to get a representation of our input data at different levels of detail. Note that this proceeding differs from the homological persistence approach introduced by Edelsbrunner et al. [4]. There are persistence pairs in $3D$ that cannot be described by a sequence $\mathscr{V}$ as shown in a counterexample by Bauer et al. [1].